Biochemical and Biophysical Research Communications 439 (2013) 23–29

Contents lists available at ScienceDirect

Biochemical and Biophysical Research Communications

journal homepage: www.elsevier.com/locate/ybbrc

A voltage-gated pore for translocation of tRNA

Sandip Koley, Samit Adhya *

Genetic Engineering Laboratory, Molecular and Human Genetics Division, CSIR-Indian Institute of Chemical Biology, 4 Raja S.C. Mullick Road, Calcutta 700 032, India

ARTICLE INFO

Article history:
Received 3 August 2013
Available online 17 August 2013

Keywords:
tRNA
Translocation
Membrane potential
AFM
Mutagenesis

ABSTRACT

Very little is known about how nucleic acids are translocated across membranes. The multi-subunit RNA Import Complex (RIC) from mitochondria of the kinetoplastid protozoon *Leishmania tropica* induces translocation of tRNAs across artificial or natural membranes, but the nature of the translocation pore remains unknown. We show that subunits RIC6 and RIC9 assemble on the membrane in presence of subunit RIC4A to form complex R3. Atomic Force Microscopy of R3 revealed particles with an asymmetric surface groove of ~20 nm rim diameter and ~1 nm depth. R3 induced translocation of tRNA into liposomes when the pH of the medium was lowered to ~6 in the absence of ATP. R3-mediated tRNA translocation could also be induced at neutral pH by a K^+ diffusion potential with an optimum of 60–70 mV. Point mutations in the Cys_2–His_2 Fe-binding motif of RIC6, which is homologous to the respiratory Complex III Fe–S protein, abrogated import induced by low pH but not by K^+ diffusion potential. These results indicate that the R3 complex forms a pore that is gated by a proton-generated membrane potential and that the Fe–S binding region of RIC6 has a role in proton translocation. The tRNA import complex of *L. tropica* thus contains a novel macromolecular channel distinct from the mitochondrial protein import pore that is apparently involved in tRNA import in some species.

1. Introduction

Translocation of cytosolic tRNAs into mitochondria occurs in a wide range of species ranging from yeast and higher plants to marsupials, primarily to complement missing or non-functional mitochondrial tRNA genes. Recent research has revealed an unexpected diversity in the nature of the protein factors involved in tRNA import in different organisms [1]. Thus, tRNA import represents a rather extreme case of convergent evolution to the process of translocating tRNA across the double mitochondrial membrane.

In yeast [2], plants [3] and trypanosomes [4,5], components of the mitochondrial protein import system are involved in tRNA import, as well as carrier proteins that are co-imported into mitochondria [6], implying the use of protein import channels for transport of tRNAs across the membranes. A tRNA binding mitochondrial complex from trypanosomes was shown to contain Tim17, a component of the inner membrane protein import machinery [4]. In contrast, in vitro tRNA import into *Leishmania tropica* mitochondria does not obligatorily require a carrier, and a functional tRNA Import Complex (RIC) from this organism lacks protein import components [7], suggesting the presence of a distinct import channel.

Native RIC contains 11 different subunits – 8 encoded in the nucleus and 3 in the mitochondrion – of which 6 are essential for import activity [8]. These include two tRNA receptors (RIC1 and RIC8A), one subunit (RIC9) that transfers tRNA from the receptor to the import pore, and three other membrane-associated proteins (RIC4A, RIC6 and RIC8B) of unknown function. RIC1 is a tRNA-dependent ATPase that provides the energy for import [9], but the mechanism of energy transduction is complex. Early work indicated that ATP hydrolysis by RIC1 results in trans-membrane proton translocation, generating a protonmotive force (p.m.f.) that drives tRNA import [10]. Subsequently, it was shown that the two components of the p.m.f. – the membrane potential ($\Delta\Psi m$) and the proton concentration gradient (ΔpH) – have distinct roles: ΔpH is required for transfer of tRNA from the receptor to RIC9, while $\Delta\Psi$ drives tRNA translocation from RIC9 through the membrane [11]. The latter observation indicates the presence of a voltage-dependent mechanism for tRNA translocation. However, the import pore is yet to be characterized.

In this study, we have reconstituted a sub-complex of RIC from three subunits (R3) that allows the transport of tRNA as well as other molecules at an optimum value of $\Delta\Psi$ generated by a pH gradient. We also demonstrate the involvement of the weekly acidic histidine residues in the Fe–S binding domain of one of the constituent domain of one of the constituent subunits in the transduction of the pH gradient. The results have implications for the mechanism of tRNA translocation.

* Corresponding author.
E-mail address: nilugrandson@gmail.com (S. Adhya).

0006-291X/$ - see front matter © 2013 Elsevier Inc. All rights reserved.
http://dx.doi.org/10.1016/j.bbrc.2013.08.036

2. Materials and methods

2.1. Purification of RIC subunits

RIC subunits and RIC6 mutants were cloned in pGEX4T1 vector (Amersham) and expressed in *Escherichia coli* BL21; recombinant fusion protein was solubilized from inclusion bodies, thrombin-digested to cleave off the GST tag, and gel-purified, as described [8]. The recombinant proteins (100 ng of gel-eluted band, suspended in 10 μl of 0.05 M Tris–HCl, pH 8.0, 0.2 M NaCl, 0.1 mM EDTA, 5 mM dithiothreitol (DTT) 0.2% SDS), were refolded by five fold dilution in buffer DB (0.2 M Tris–HCl, pH 7.5, 5 mM $MgAc_2$, 1 mM DTT, 0.1 mM phenylmethylsulphonyl fluoride (PMSF), 10% glycerol), on ice for 2 h and then concentrated by ultrafiltration in a Microcon 10 unit (Amicon).

2.2. Reconstitution of RIC sub-complexes

Phosholipid vesicles were prepared from phosphatidyl choline by dialysis against 5 mM HEPES-KOH, pH 7.5, 5 mM MgAc2, 20 mM KCl for 18 h at 4 °C [12]. Complexes were assembled using refolded subunits (10–15 ng each) in buffer DB with or without liposomes (500 μg) in 20 μl, incubated for 2 h on ice. R3 was reconstituted with subunits RIC4A, RIC6 and RIC9; R6 contained, additionally, RIC1, RIC8A and RIC8B.

2.3. Blue native PAGE

Mitochondrial respiratory complexes were solubilized according to Schagger's protocol [13] from purified mitochondria of the human HepG2 cell line (200 μg of protein), with BAM buffer (50 mM BisTris–HCl, pH 7.0, 0.75 M ε-aminocaproic acid, 2% dodecyl maltoside) for 45 min at 4 °C. The mitochondrial extract was purified by centrifugation and concentrated to 10 μl per 200 μg protein by Microcon 30 ultrafiltration. Assembled complexes were adjusted to 62 mM Tris–HCl, pH 6.8, 2.5% β-mercaptoethanol, 75 mM DTT, 7.5% glycerol, 0.005% bromophenol blue before loading on the gel. Electrophoresis was carried out on 5–15% gradient polyacrylamide gels, followed by Coomassie staining.

2.4. Atomic Force Microscopy (AFM)

R3, reconstituted as above, was diluted to 1 ng of each subunit/μl in PBS, and 10 μl of the sample was deposited onto freshly cleaved muscovite Ruby mica sheets (ASTM V1 Grade Ruby Mica from MICAFAB, Chennai) for 10–30 min. The sample was gently washed with 0.5 ml MilliQ water, and imaging was done in dry mode. AAC mode AFM was performed using a Pico plus 5500 AFM (Agilent Technologies USA) with a piezo scanner having a maximum range of 9 μm. Micro-fabricated silicon cantilevers of 225 μm length with a nominal spring force constant of 21–98 N/m were used from Nano sensors. Cantilever oscillation frequency was tuned into resonance frequency. The cantilever resonance frequency was 150–300 kHz. Images (256 by 256 pixels) were captured with a scan size of 600–1000 nm at the scan speed rate of 1.083 μm/s. Images were processed by flatten using Picovew1.10.1 (9995) software (Agilent Technologies USA). Image interpretation was performed through Pico Image Advanced Version 5.1.1.5944, 2011.

2.5. Particle size estimation

A topographic profile analysis (Fig. 1) was performed on individual particles, as described for the nuclear pore complex [14]. Particle diameter was taken as the difference in the *x*-coordinate between the start and end of the profile. The channel rim diameter was the inter-peak distance x2–x1. Channel depth (d1, d2) was the difference between the peak and trough heights. The pore diameter was taken as the channel width at half-depth (i.e., 0.5 × d1 or d2, whichever is greater).

2.6. Preparation of tRNA

^{32}P-labeled $tRNA^{Tyr}$ (GUA) transcript was prepared by run-off transcription of linearized plasmid pSKB1 by T7 polymerase, as described [12] DNA oligonucleotides and EcoRI-linearized plasmid pGEM4Z (Promega) were 5′-end labeled with γ-^{32}P-ATP and T4 polynucleotide kinase. γ-^{32}P-ATP (3000 Ci/mmol) and ^{35}S-methionine (1100 Ci/mmol) were from Perkin Elmer.

2.7. Translocation assays

In the standard ATP-dependent reaction, reconstituted liposomes (5 μl, internal pH 7.5) were incubated with ^{32}P-labeled RNA (50 fmol), or 10 μCi of γ-^{32}P-ATP, or 10 μCi of ^{35}S-methionine, or 12.5 pmol of oligodeoxynucleotide, or ~1 pmol plasmid DNA, in 10 μl of import buffer (10 mM Tris–HCl [pH 7.5], 10 mM $MgCl_2$, 1 mM DTT, and 4 mM ATP) at 37 °C for 15 min. Otherwise, ATP was omitted and the incubation carried out in Tris or sodium phosphate buffers of indicated pH, or at pH 7.5 in presence of indicated KCl concentrations and 1 mM valinomycin. RNAse A + T1 resistant RNA was recovered from the washed liposomes, and analyzed by urea–PAGE. RNA was quantified by phosphor imaging, autoradiography and scintillation counting of dried gel bands. Membrane potentials ($\Delta\Psi$ at a given external pH or K^+ concentration were calculated on the basis of the Nernst equation [15].

2.8. Molecular modeling

The *L. tropica* RIC6 (gene id LmjF35.1540 in the *Leishmania major* genome sequence database: http://www.genedb.org/genedb/leish/index.jsp) was shown to be identical to the Complex III Reiske Iron Sulfur protein (ISP) on the basis of sequence and homology modeling [9]. Critical residues of the Fe–S cluster were identified in the SwissProt homology model (www.expasy.ch/swissmod/SWISSMODEL.html) and residue interactions of the Fe–S cluster were displayed using ChemDraw.

2.9. Site-directed mutagenesis

The plasmid pGEX4T1 carrying the wild type *L. tropica* RIC6 gene, was purified from *E. coli* XL1-Blue (Dam methylase positive), and used for site-directed mutagenesis to produce mutant versions of all the cysteine and histidine residues of the protein, using the Stratagene QuikChange site-directed mutagenesis kit. The expression plasmid was amplified by PCR using Pfu Turbo DNA polymerase (Stratagene), in the presence of the (+) and (−) strand mutagenesis primers (Supplementary Table S1). The methylated wild-type sequence was selectively digested with Dpn I (New England Biolabs), and the mutant plasmids amplified by transformation of *E. coli* XL1-Blue. Mutations were confirmed by direct sequencing of both strands.

3. Results

3.1. Reconstitution of sub-complex R3

We have shown previously that sub-complexes derived from native RIC, containing 6 (R6) or eight (R8) of the nucleus-encoded subunits, can be reconstituted from bacterially expressed proteins, and that these sub-complexes retain full import activity [8]. Two of

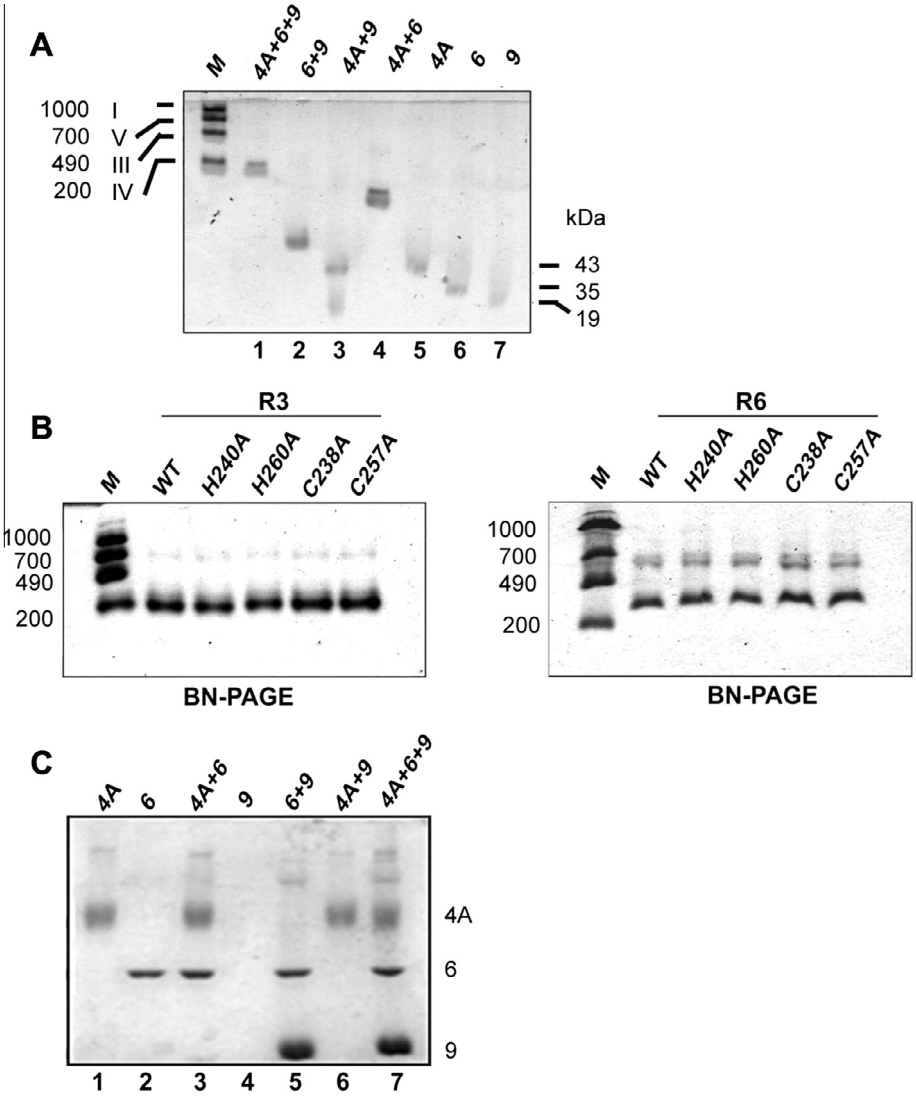

Fig. 1. Reconstitution of RIC sub-complexes. (A and B) Blue Native PAGE of complexes assembled with the indicated combinations of subunits (panel A, lanes 1–4), or with a combination of RIC4A, RIC9 and either wild-type or mutant RIC6 (panel B, left), or with RIC1, RIC4A, RIC8A, RIC8B, RIC9 and either wild type or mutant RIC6 (panel B, right). M, mitochondrial respiratory complexes run as size markers (molecular masses indicated at left). (C) Complexes were assembled with the indicated combinations of RIC4A, RIC6 and RIC9 in presence of liposomes, the liposomes washed, detergent extracted and the proteins run on SDS PAGE. The identities and sizes of the different subunits are indicated at the right.

the non-receptor subunits, RIC6 and RIC9, form a heterodimer, and 3 copies of each subunit are present in the native complex [8,11]. Another essential subunit RIC4A, a kinetoplastid-specific protein of unknown structure [8], was predicted by the PredictProtein program to have a 74% α-helical content with a single-trans-membrane helix. When these three subunits were combined, a complex R3 of estimated size 200 kDa was observed by Blue native gel electrophoresis (Fig. 1A, lane 1; the presence of a doublet band may be due to different conformations resolved in this gel system). Omitting RIC4A resulted in formation of a smaller RIC6–RIC9 complex of apparent size 70 kDa (Fig. 1A, lane 2), corresponding to a stoichiometry of 1:1–2 (based on molecular masses of RIC6 and RIC9). No complex was formed in the absence of RIC6 (Fig. 1A, lane 3). In the absence of RIC9, a RIC4A: RIC6 complex of apparent mass 151 kDa was formed, corresponding to a stoichiometry of 1:3, indicating that RIC4A-induced trimerization of RIC6 (Fig. 1A, lane 4). The mass of R3 corresponded to the composition $(RIC4).(RIC6)_3.(RIC9)_3$. The 200-kDa R3 sub-complex, as well as the larger R6, were also formed when the reconstitution was carried out with various point mutants of RIC6 in place of wild-type protein (Fig. 1B). In both cases, a larger complex corresponding to a dimer or trimer, was observed (aggregates were also evident by Atomic Force Microscopy, see Fig. 2B).

In a different approach, complexes were assembled on phospholipid vesicles, and the composition of lipid-bound proteins assessed by SDS–PAGE (Fig. 1C). Either RIC4A or RIC6, but not RIC9, could directly associate with the membrane (Fig. 1C, lanes 1 and 2). Assembly of RIC9 required the presence of RIC6 (Fig. 1C, lanes 3–5).

Taken together, these results support an assembly pathway consisting of independent insertion of RIC4A and RIC6 into the membrane, formation of RIC6–RIC9 heterodimers and their trimerization in presence of RIC4A to form the sub-complex R3.

3.2. Atomic Force Microscopy (AFM) of R3

The R3 complex was visualized by AFM (Fig. 2A and B). Spherical particles of diameter 53.82 + 16.17 nm (n = 50) were observed. About 60% of the particles had a groove or channel of outer rim diameter 20.57 + 8.19 nm (n = 25). In cross section, the groove appeared asymmetrical, i.e., of greater depth on one side (1.33 + 0.4 vs. 0.824 + 0.4 nm (n = 10)), with the channel diameter at half depth being 14.4 + 2.88 nm (n = 10) (Fig. 2C). No such channel

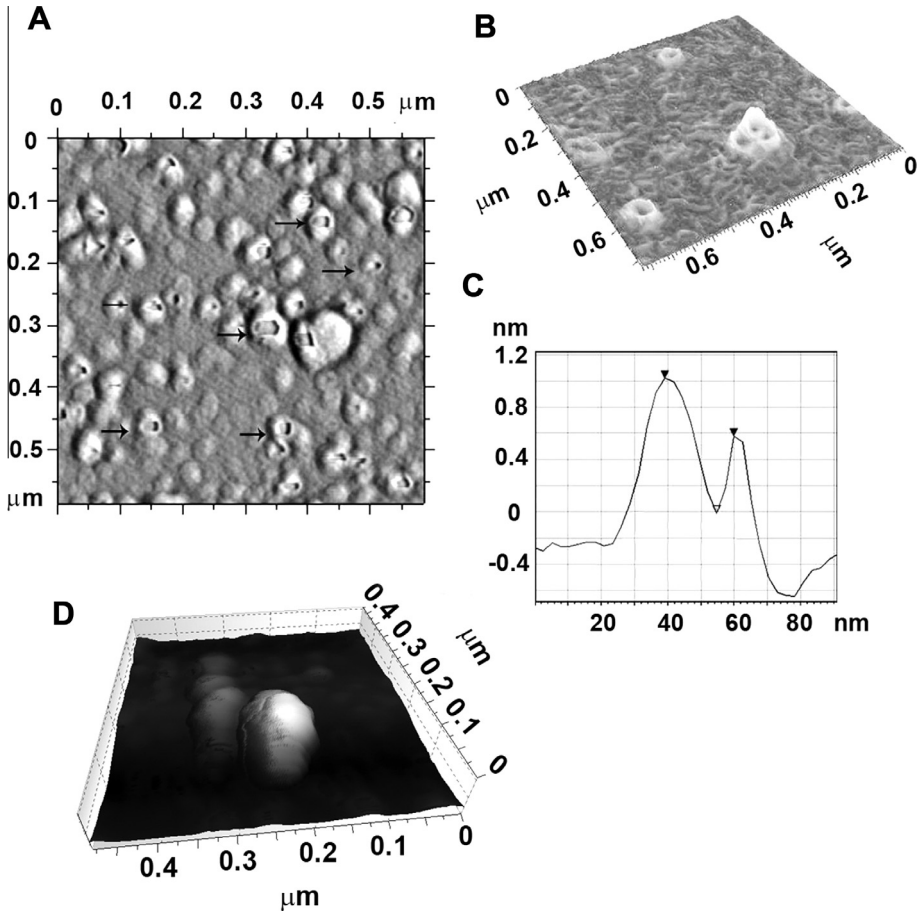

Fig. 2. Atomic Force Microscopy of R3 sub-complex. (A) 2-d view showing particles with pores (arrow). (B) 3-d view of monomeric and a trimeric comlex with pores. (C) Profile analysis of a single particle showing the unequal depths on either side of the groove. (D) Complex formed with RIC4A and RIC6 (in absence of RIC9).

was observed in particles assembled with only RIC4A and RIC6 (Fig. 2D), showing the contribution of RIC9 to channel formation.

3.3. tRNA translocation by R3 at acidic pH

To assess the functionality of sub-complex R3, R3-reconstituted proteoliposomes were incubated with radiolabeled tRNA under various conditions, and import was monitored by RNAse protection. In contrast to the ATP-dependent import observed with larger sub-complexes R6 and R8 [8], there was no import induced by R3 at pH 7.5 in presence of ATP (Fig. 3A, lane 4). However, acidification to pH 6 resulted in tRNA import into phospholipid vesicles in the presence or absence of ATP (Fig. 3A, lanes 2 and 3).

When different combinations of RIC4A, RIC6 and RIC9 were assembled on liposomes, it was observed that only R3, containing all 3 subunits, was active in tRNA import at acidic pH (Fig. 3B), confirming that R3 is the minimum functional unit for translocation.

The efficiency of tRNA import rose sharply between pH 7.5 and pH 6.5, and was maintained down to pH 5.0 (Fig. 3C). In all cases the internal pH of the vesicles was 7.5. These results indicated the formation of a minimal pore complex that allowed the passage of tRNA upon acidification of the external pH to 5–6, resulting in formation of a trans-membrane $\Delta\Psi$ of 30–90 mV.

The ΔpH and/or $\Delta\Psi$ components of trans-membrane proton-motive force can be inhibited by inhibitors and uncouplers of mitochondrial respiration. The protonophore CCCP, which disperses the proton gradient, thereby inhibiting both components, inhibited R3-induced tRNA import at pH 6 (Fig. 3D, lane 3). Import was also sensitive to the K^+ ionophore valinomycin in presence of 0.1 M K^+, but insensitive to the Na^+/H^+ exchanger nigericin (Fig. 3D, lanes 4 and 5). At high external K^+ concentration, valinomycin would promote import of K^+ into the vesicle, thereby altering the pH-induced $\Delta\Psi$, whereas nigericin would effect an electro-neutral exchange of H^+ with Na^+, thereby specifically affecting ΔpH. These results therefore indicate that membrane potential generated by acidification drives import through R3.

3.4. R3-induced translocation in presence of a K^+ diffusion potential

The role of $\Delta\Psi$ was directly tested by incubating the R3-liposomes (with a constant internal K^+) in pH-neutral buffers of different external K^+ concentrations, in presence of valinomycin to allow the K^+ to diffuse across the membrane down the concentration gradient, thereby generating a potential difference that depends on the ratio of the internal to external K^+ concentrations [16]. By progressively narrowing down the range of external K^+ concentrations, it was possible to determine the optimal diffusion potential for import. These titration experiments (Fig. 3E and F) showed that tRNA import occurred in the range 0.5–8 mM K^+, with a peak at 2 mM K^+. The internal K^+ being 20 mM, the peak (Fig. 3F) corresponds to a $\Delta\Psi$ of ~60 mV. This corresponds to the threshold value of 59.1 mV at pH 6 observed by pH titration (Fig. 3C). These results establish that the R3 forms a membrane pore that is gated primarily by the trans-membrane potential $\Delta\Psi$.

3.5. Role of RIC6 in proton-driven tRNA translocation

The opening of the R3 channel at acidic pH implies the presence of a proton path, i.e. residues that participate in proton translocation during channel opening. To identify such residues we initially

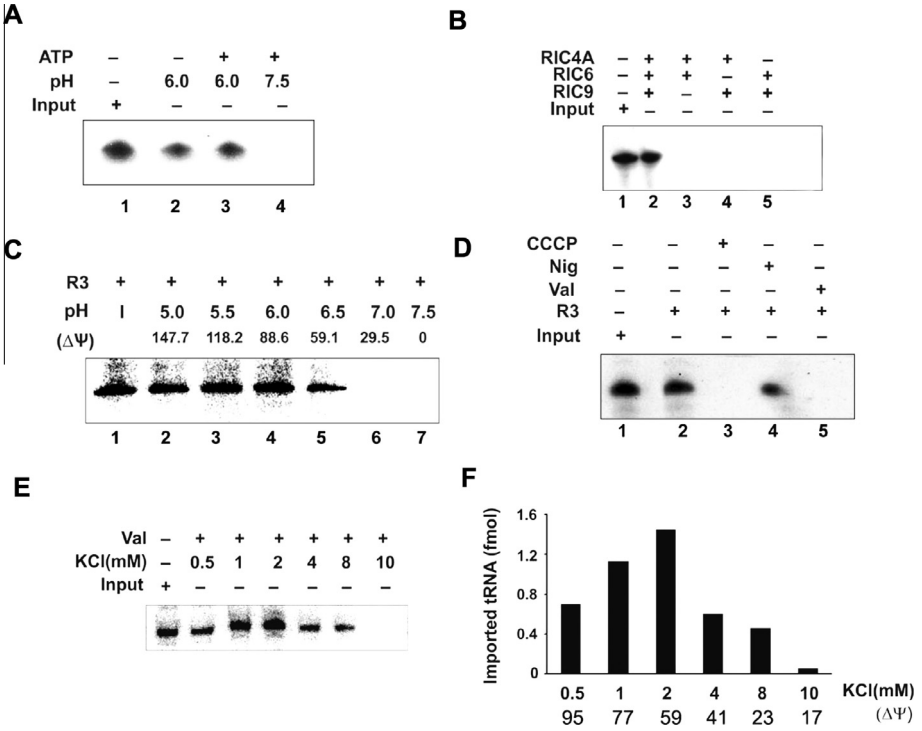

Fig. 3. R3-induced tRNA import is driven by membrane potential. (A–E) R3-proteoliposomes were incubated with ^{32}P-labeled tRNA^{Tyr} (GUA) transcripts in buffers of indicated pH in absence or presence of ATP. (A) Effect of acidification to ph 6.0. (B) Effect of subunit composition of the complex on tRNA import at pH 6.0. (C) Effect of varying pH on import. (D) Effect of CCCP, nigericin (Nig) or valinomycin plus 1 M K^+ (Val) on R3-induced import at pH 6.0. (E) and (F) R3-induced tRNA import driven by a K^+ diffusion potential. (E) R3-proteoliposomes were incubated with ^{32}P-labeled tRNA^{Tyr}(GUA) transcripts at pH 7.5 in presence of the indicated external K^+ concentration and valinomycin. (F) Quantification of tRNA import at different external K^+ concentrations. Calculated $\Delta\psi$ values are indicated.

focused on subunit RIC6. RIC6 is homologous to the Fe–S protein (ISP) subunit of respiratory Complex III [9]. The homology model of RIC6 shows the presence of a globular domain that binds the $(Fe–S)_2$ prosthetic group via coordination with Cys238, His240, Cys257 and His260 (Fig. 4A and B). These and other Cys and His residues were individually mutated to Ala and used to reconstitute R3 complexes on liposomes. Normal-sized R3 complexes were formed with all of the mutants, implying that assembly of the complex is not affected (Fig. 1). Mutants H116A, H228A, H263A, H293A, C243A and C259A supported ATP-dependent import induced by R6 at pH 7.5, as well as ATP-independent import by R3 at pH 6, while mutants H240A, H260A, C238A and C257A were inactive under both conditions (Fig. 4C and D). Significantly, all mutants that were inactive at pH 6 were active in R3-induced import under a K^+-diffusion potential (Fig. 4E). These results indicate that the His and Cys residues in the Fe–S binding domain of RIC6 are involved in proton transactions, but not in $\Delta\Psi$-induced channel opening.

4. Discussion

Although tRNA translocation has been studied for a number of years in a variety of species, the detailed molecular mechanism remains largely unknown, particularly with regard to the nature of the translocation channel. In this report we present the first evidence for a voltage-gated minimal translocation pore of RIC, constituted by RIC6, RIC9 and RIC4A. Sub-complex R3 retains many of the characteristics of import observed earlier with intact mitochondria, or with liposomes reconstituted with the native or reconstituted RIC: (1) As observed earlier with native RIC [10,11], the channel in R3 was opened for the passage of tRNAs at acidic pH in the range of 5–6. (2) Both RIC- and R3-catalyzed translocation at pH 6 was sensitive to protonophores and to valinomycin/K^+, reagents that disperse the membrane potential $\Delta\Psi$, but resistant to nigericin, which lowers ΔpH; with native RIC, nigericin inhibits the transfer of tRNA from the receptor to RIC9 prior to channel opening [11]. We show here that R3 channel opening could also be induced by a K^+-diffusion potential at an optimum $\Delta\Psi$ of ~60 mV (Fig. 3). (3) Mutations in RIC6 have identical effects on ATP-dependent, receptor-mediated import by R6 and the pH dependent import by R3 (Fig. 4). Thus the R3 pore likely represents the true pore complex within the native import complex.

Atomic Force Microscopy revealed that R3 consists of particles with a pronounced surface groove (Fig. 2). The channel diameter of 10–20 nm is considerably higher than that of the protein import channel or the endoplasmic reticulum protein translocase (2 nm) and is capable of accommodating the L-shaped tRNA molecule with an end-to-end distance of 8 nm, but is smaller than the ~50 nm groove on the cytosolic surface of the Nuclear Pore Complex [14]. Moreover, in contrast to the other pores, which are symmetric, the R3 groove is asymmetric; this may be due to the presence of the single copy of RIC4A that acts a nucleus for assembly of the pore complex.

In this report we have explored the function of RIC6 through mutagenesis of a number of Cys and His residues in the molecule. Of these, only Cys238, His240, Cys257 and His260, all within the globular Fe–S binding domain were found to be essential. Mutations at equivalent His residues in a bacterial ISP affect binding of the Fe–S group, resulting in an inactive Complex III that is leaky to protons; it has been suggested that the Fe–S cluster acts as a proton exiting gate [17]. It is interesting that opening of the R3 channel starts to occur at pH ~6.5, a value close to the pKa of the histidine imidazole ring. At this pH protonation and deprotonation of the imidazole moiety are equally probable, and thus the relay of protons through the molecule is facilitated. The pKa of Cys is 8.2, thus at pH 6 it will exist mostly in the protonated (SH) form.

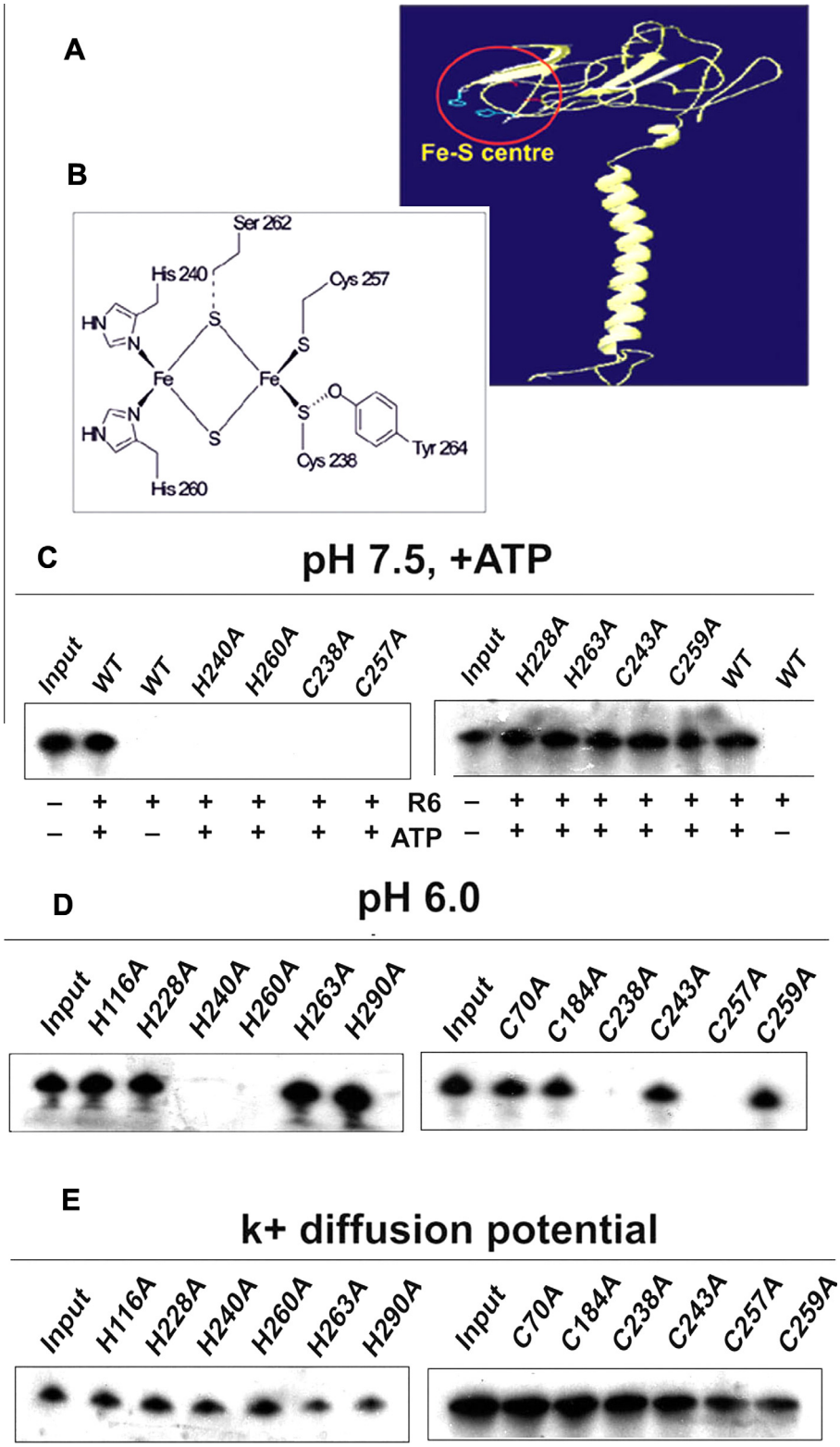

Fig. 4. Role of RIC6 in pH-driven import. (A) Homology modeled structure of RIC6/ISP. The conserved portion of RIC6 is shown, including the N-terminal α helix and the globular Fe–S binding domain. (B) Modeled interactions between the Cys and His residues and the Fe–S prosthetic group. (C)–(E) Effect of mutations on import activity of proteoliposomes reconstituted with R6 (C) or R3 (D and E) containing wild-type or indicated mutants of RIC6. (C) pH 7.5, +ATP. (D) pH 6.0. (E) pH 7.5 in presence of I mM K^+ plus valinomycin.

Given the proximity of the Cys and His side chains within the Fe–S binding domain (Fig. 4), it is possible that the Cys SH group hydrogen bonds with the histidine N atom to stabilize the orientation of the imidazole group for proton relay.

Import of tRNA through the R3 pore is similar to import of proteins through the mitochondrial protein import pore in requiring $\Delta\psi$ [16], but there is electrophysiological evidence against voltage sensitivity of the latter [18], and the membrane potential is

believed to drive the electrophoretic movement of the polypeptide chain through the pore. In contrast to protein import, which increases linearly with the magnitude of $\Delta\psi$, the minimum value depending on the import substrate [16], import through R3 occurs at an optimum value of $\Delta\psi$ (Fig. 3), as expected of voltage-driven channel opening. Thus, the tRNA import pore of *L. tropica* represents, to our knowledge, the first instance of a voltage-gated macromolecule membrane channel.

Acknowledgments

Supported by CSIR Network Project NWP0038. S.K. received a CSIR Senior Research Fellowship. We thank T. Muruganandan for Atomic Force Microscopy.

Appendix A. Supplementary data

Supplementary data associated with this article can be found, in the online version, at http://dx.doi.org/10.1016/j.bbrc.2013.08.036.

References

[1] A.M. Duchene, C. Pujol, L. Marechal-Drouard, Import of tRNAs and aminoacyl-tRNA synthetases into mitochondria, Curr. Genet. 55 (2009) 1–18.
[2] I. Tarassov, N. Entelis, R.P. Martin, An intact protein translocating machinery is required for mitochondrial import of a yeast cytoplasmic tRNA, J. Mol. Biol. 245 (1995) 315–323.
[3] T. Salinas, A.M. Duchene, L. Delage, S. Nilsson, E. Glaser, M. Zaepfel, L. Marechal-Drouard, The voltage-dependent anion channel, a major component of the tRNA import machinery in plant mitochondria, Proc. Natl. Acad. Sci. U.S.A. 103 (2006) 18362–18367.
[4] D. Seidman, D. Johnson, V. Gerbasi, D. Golden, R. Orlando, S. Hajduk, Mitochondrial membrane complex that contains proteins necessary for tRNA import in *Trypanosoma brucei*, J. Biol. Chem. 287 (2012) 8892–8903.
[5] F. Tschopp, F. Charriere, A. Schneider, In vivo study in *Trypanosoma brucei* links mitochondrial transfer RNA import to mitochondrial protein import, EMBO Rep. 12 (2011) 825–832.
[6] I. Tarassov, N. Entelis, R.P. Martin, Mitochondrial import of a cytoplasmic lysine-tRNA in yeast is mediated by cooperation of cytoplasmic and mitochondrial lysyl-tRNA synthetases, EMBO J. 14 (1995) 3461–3471.
[7] S. Adhya, Leishmania mitochondrial tRNA importers, Int. J. Biochem. Cell Biol. 40 (2008) 2681–2685.
[8] S. Mukherjee, S. Basu, P. Home, G. Dhar, S. Adhya, Necessary and sufficient factors for the import of transfer RNA into the kinetoplast mitochondrion, EMBO Rep. 8 (2007) 589–595.
[9] S. Goswami, S. Adhya, The alpha-subunit of Leishmania F1 ATP synthase hydrolyzes ATP in presence of tRNA, J. Biol. Chem. 281 (2006) 18914–18917.
[10] S.N. Bhattacharyya, S. Adhya, TRNA-triggered ATP hydrolysis and generation of membrane potential by the leishmania mitochondrial tRNA import complex, J. Biol. Chem. 279 (2004) 11259–11263.
[11] S. Basu, S. Mukherjee, S. Adhya, Proton-guided movements of tRNA within the Leishmania mitochondrial RNA import complex, Nucleic Acids Res. 36 (2008) 1599–1609.
[12] S.N. Bhattacharyya, S. Chatterjee, S. Goswami, G. Tripathi, S.N. Dey, S. Adhya, "Ping-pong" interactions between mitochondrial tRNA import receptors within a multiprotein complex, Mol. Cell. Biol. 23 (2003) 5217–5224.
[13] I. Wittig, H.P. Braun, H. Schagger, Blue native PAGE, Nat. Protoc. 1 (2006) 418–428.
[14] V. Shahin, L. Albermann, H. Schillers, L. Kastrup, C. Schafer, Y. Ludwig, C. Stock, H. Oberleithner, Steroids dilate nuclear pores imaged with atomic force microscopy, J. Cell Physiol. 202 (2005) 591–601.
[15] A. Dawson, M. Klingenberg, R. Kramer, Transport across membranes, in: V.M. Darley-Usmar, D. Rickwood, M.T. Wilson (Eds.), Mitochondria: A Practical Approach, IRL Press, Oxford, 1987, pp. 35–78.
[16] J. Martin, K. Mahlke, N. Pfanner, Role of an energized inner membrane in mitochondrial protein import Delta psi drives the movement of presequences, J. Biol. Chem. 266 (1991) 18051–18057.
[17] B. Gurung, L. Yu, D. Xia, C.A. Yu, The iron–sulfur cluster of the Rieske iron–sulfur protein functions as a proton-exiting gate in the cytochrome bc(1) complex, J. Biol. Chem. 280 (2005) 24895–24902.
[18] O. Moran, G. Sandri, E. Panfili, W. Stuhmer, M.C. Sorgato, Electrophysiological characterization of contact sites in brain mitochondria, J. Biol. Chem. 265 (1990) 908–913.